International Journal of Mechanical, Industrial and Aerospace Sciences
ISSN: 2517-9950
Vol:9, No:4, 2015

Multidisciplinary and Multilevel Design Methodology of Unmanned Aerial Vehicles Using Enhanced Collaborative Optimization

Pedro F. Albuquerque, Pedro V. Gamboa, Miguel A. Silvestre

***Abstract*—**The present work describes the implementation of the Enhanced Collaborative Optimization (ECO) multilevel architecture with a gradient-based optimization algorithm with the aim of performing a multidisciplinary design optimization of a generic unmanned aerial vehicle with morphing technologies. The concepts of weighting coefficient and dynamic compatibility parameter are presented for the ECO architecture. A routine that calculates the aircraft performance for the user defined mission profile and vehicle's performance requirements has been implemented using low fidelity models for the aerodynamics, stability, propulsion, weight, balance and flight performance. A benchmarking case study for evaluating the advantage of using a variable span wing within the optimization methodology developed is presented.

***Keywords*—**Multidisciplinary, Multilevel, Morphing, Enhanced Collaborative Optimization (ECO).

I. Introduction

AERONAUTICAL design involves a comprehensive analysis of a wide range of mutually interacting phenomena, requiring a sound knowledge on disciplines like materials, aerodynamics, structures, fluid-structure interactions, control, stability, performance, among others, thus being an inherently multidisciplinary task. Indeed, aircraft design is commonly regarded as a separate design discipline [1], which is different from the former in the way that the designer needs to be well versed in all of them.

Multidisciplinary design optimization (MDO) is doubtlessly of utmost relevance in this context, hence a topic of intense research. The possibilities MDO methodologies unfold show that they will definitely pave the way of engineering design in a range of subjects that goes far beyond the aerospace industry.

There have been a number of surveys of MDO over the last two decades. Haftka et al [2] were among the first to review the MDO architectures known at the time. Cramer et al [3] formalized the monolithic architectures and detailed the required gradient computation methods. Balling and Sobieski [4] identified a number of possible monolithic approaches and estimated their computational cost. In a collection of articles Alexandrov and Hussaini [5] also gave their contribute. Kroo [6] provided a comprehensive overview of MDO, including a description of both monolithic and distributed architectures. In the same volume, Alexandrov [7] discussed the convergence properties of certain partitioning strategies for distributed architectures, and Balling [8] focused on partitioning as a way to provide disciplinary autonomy. Sobieski and Haftka [9] published an exhaustive survey of the MDO literature.

However, the most recent survey was made by Martins et al [10] where all the optimization architectures known by the time of its publication have been presented. In this review, all the architectures known at the time have been compared using a unified description, not only being the latest but also the most comprehensive effort towards a straightforward comparative evaluation of the existing methodologies.

A primary motivation for decomposing the MDO problem comes from the inherent architecture of the engineering design

Pedro F. Albuquerque is a Researcher and PhD Candidate at the Department of Aerospace Sciences, University of Beira Interior, Covilhã, Portugal (e-mail: pffa@ubi.pt).

Pedro V. Gamboa is an Assistant Professor at the Department of Aerospace Sciences, University of Beira Interior, Covilhã, Portugal (e-mail: pgamboa@ubi.pt).

Miguel A. Silvestre is an Assistant Professor at the Department of Aerospace Sciences, University of Beira Interior, Covilhã, Portugal (e-mail: mars@ubi.pt).

Nomenclature

b	wingspan	ν	kinematic viscosity
c	wing chord	Δ	interval or variation
C_d	2D drag coefficient	Λ	aspect ratio
C_l	2D lift coefficient		**Subscripts**
C_m	2D pitching moment coefficient	cb	climb
D_{fus}	fuselage diameter	cz	cruise
E	energy	dt	descent
L_{fus}	fuselage length	ene	energy
L_m	main gear length	eng	engine
L_n	nose gear length	fus	fuselage
N	propeller rotational velocity	max	maximum
p	span extension factor	min	minimum
P	power	mlg	main landing gear
R	range	mot	motor
RoC	rate-of-climb	nlg	nose landing gear
S	area	pay	payload
t/c	airfoil relative thickness	$prop$	propeller
V	velocity	ref	reference
W	weight	req	required
β	sideslip angle	to	take-off
δ	thrust setting	vt	vertical tail
η	efficiency	w	wing
λ	taper ratio		

environment itself, which usually involves breaking up the design of large systems and distributing it between several different design groups, which are often geographically apart and communicate seldom. Moreover, they will probably have different internal procedures and optimization methodologies. The idea behind distributed architectures is to mimic the natural divisions found in design companies, conversely to what happens in the so-called monolithic architectures - those that solve a single optimization problem.

Another key area of research are morphing technologies, notwithstanding that the development of these mechanisms is not new and can be traced back to even before the first (heavier-than-air) successful flight [11]. Nonetheless, in recent decades, there has been an ever-growing academic, civil and military interest in these technologies [12] which has contributed to an improvement in the overall aircraft performance and multimission capabilities [13].

Morphing technologies, which have been described by Barbarino [12] can be: airfoil changes, like camber and thickness, and wing layout changes, like chord length, sweep and span (in the wing plane), and torsion and dihedral (out of the wing plane). The use of morphing has been growing as it can definitely contribute to lower operational costs and increase the aircrafts' flight envelopes enabling the same airplane to perform different missions with a high level of performance.

Several different approaches are available for performing MDO. Parametric studies enable researchers to swiftly infer about how the most relevant variables influence key objective functions by allowing the assessment of the design domain as a whole [14]. Conversely, multilevel optimization architectures differ from the former in that a single design point is being computed at each iteration. The methodology presented uses the latter approach and shows how it is possible to take advantage of a synergy between the use of multidisciplinary design optimization and morphing wing technologies to get meaningful improvements of the overall aircraft performance.

II. Enhanced Collaborative Optimization

After a comprehensive performance benchmark study of the already developed optimization architectures [10], it has been decided to implement the most recent version of Collaborative Optimization (CO) which has been named Enhanced Collaborative Optimization (ECO) and has been presented by Roth and Kroo [15]–[17].

A. Collaborative Optimization

Collaborative optimization is a method for the design of complex, multidisciplinary systems that was originally proposed [18] in 1994. CO is one of several decomposition-based methods that divides a design problem in disciplinary optimization subspaces - the so-called distributed architectures [10].

With respect to the original CO formulation, the system and discipline optimization have been reversed in ECO: the system subproblem minimizes system infeasibility while the discipline subproblems minimize the system objective. This is an unconstrained problem and its post-optimality derivatives are not required by the system subproblem because the system subproblems are treated as parameters. ECO has shown to be effective in reducing the number of discipline analyses when compared to CO [15], [17] and to compare favorably with the methods against which it has been bench-marked [10], [16], [19]–[22].

B. ECO Formulation

1) System Level Optimization: In ECO, the system level optimization is simply an unconstrained minimization problem. The global objective function (i.e. the ultimate design goal) is not present in the system level objective. The system level single goal is to achieve compatibility between subspaces (1).

$$\text{Min } J_{sys} = \sum_{i=1}^{n} \lambda_w^i \sum_{j=1}^{n_{si}} (z_j - {x_s}_j{}^{*(i)})^2 \tag{1}$$

subject to No constraints

where z are the system level targets for shared variables.
x^* represents the subspace best attempt to match the system level targets, (subject to local constraints).
λ_w^i is a weighting coefficient which will be different for each subspace.
n number of subspaces.
n_{si} is a the number of shared variables in subspace i.

2) Subspace Level Optimization: The subspaces are responsible for most of the design decisions. Their objective function includes three components: a local objective function (which will generically depend on both global and local variables), a compatibility term (with a quadratic measure of compatibility) and a feasibility term (with a set of slack variables) (2).

$$\begin{aligned}\text{Min } J_i =& F(x_S, x_L) + \lambda_C^* \sum_{k=1}^{n_{s_i}} (x_{s_k} - z_k)^2 \\ &+ \lambda_F \sum_{j=1}^{n} \left[\sum_{k=1}^{n_{g_j}} (s_{g_k}^{(j)}) + \sum_{l=1}^{n_{h_j}} (s_{h_l}^{(j)} + e_l^{(j)}) \right]\end{aligned} \tag{2}$$

subject to
$g_k^{(i)}(x_S, x_L) \geq 0, k = 1...n_{g_i}$
$h_l^{(i)}(x_S, x_L) = 0, l = 1...n_{h_i}$
$\tilde{g}_k^{(j)}(x_s) + s_{g_k}^{(j)} \geq 0, j = 1...n, k = 1...n_{g_j}, j \neq i$
$\tilde{h}_l^{(j)}(x_s) + s_{h_l}^{(j)} - e_l^{(j)} = 0, j = 1...n, l = 1...n_{h_j}, j \neq i$
$s_g, s_h, e \geq 0$

where F is the local objective function.
λ_C^* is a dynamic compatibility parameter.
λ_F is a feasibility parameter.
n_{gj} is the number of inequality constraints in subspace j.
n_{hj} is the number of equality constraints in subspace j.
$\tilde{g}_k^{(j)}$ is a linear model of the k^{th} inequality constraints in subspace j.
$\tilde{h}_l^{(j)}$ is a linear model of the l^{th} equality constraints. in subspace j

C. Remarks

In order to validate the implemented ECO architecture the Analytical Test Case [15] and the Rosenbrock Problem [16] shown by Roth et al have been reproduced. The obtained results agree with the ones presented in these two publications.

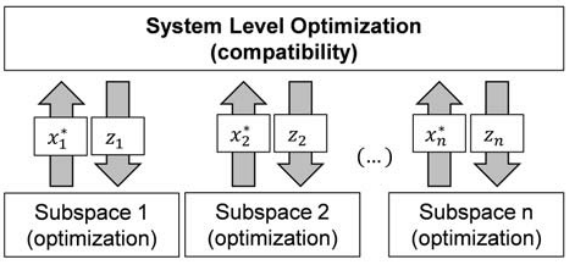

Fig. 1 Schematic representation of the Enhanced Collaborative Optimization architecture

There have been two significant modifications to the original ECO formulation [15], the first being the use of a weighting coefficient (λ_w^i) on the system level optimization problem (1) which enables a differential weighting of the squared differences between the system level targets and the respective subspaces converged solutions. The other relevant difference from the works presented to date [15], [16], [23], is that the compatibility parameter is a dynamic quantity. This is because it as been found that an early compatibility between subspaces may jeopardize the actual multilevel optimization problem. In order to mitigate this shortcoming on the first system level iterations each disciplinary (subspace) optimization is fully independent ($\lambda_C^* = 0$) and only after a threshold number of system level iterations does the compatibility term become active ($\lambda_C^* > 0$).

The third term in (2) is called the feasibility term and is used to make sure that the equality and inequality constraints imposed in each subspaces are known in other subspaces. The first part of the term refers to inequality constraints whilst the second refers to the equality constraints. Both terms will be null if the subspace problem under consideration is unconstrained.

As it is common in engineering applications, the design variables may have diverse ranges, with quantities having different orders of magnitude. A small variation of the greater ones may thus have a much more significant impact on the subspaces objective functions and respective gradients. In order to obviate this problem, a normalization method [23] to avoid the fluctuations caused by sensitive design variables has been adopted (3), where (x) is a generic design variable.

$$x_{norm} = \frac{x - x_{min}}{x_{max} - x_{min}} \tag{3}$$

III. Optimization Algorithm

The main purposes of this research have been the multilevel optimization architecture implementation and the physical models development. Due to that fact, the authors have decided not to generate their own optimization algorithm, having opted to use a previously developed gradient-based method.

The implemented algorithm is based on a sequential equality constrained quadratic programming method. It uses a slightly modified version of the Pantoja-Mayne update for the Hessian of the Lagrangian, variable dual scaling and an improved Armijo-type step size algorithm. Bounds on the variables are treated in a gradient projection like fashion [24], [25].

IV. Methodology

A. Variable Span Wing

In order to demonstrate the profitability of morphing wing concepts in the context of MDO, and among the many morphing wing concepts developed at present time the choice has been to assess the advantages of using a variable span wing compared to a fixed wing. This choice has been based on two fundamental reasons. Firstly, this is clearly one of the morphing wing solutions that produces most significant performance impacts as the lifting surface area and aspect ratio are parameters of paramount relevance. Secondly, the fact that in-house developments of such a concept have already proven successful [26], [27] and the development of a weight estimate correlation [28] for variable span wings have further supported this choice.

B. Optimization Methodology

To show the validity of the implemented optimization methodology, the overall optimum aircraft layout, and, more specifically, the wing sizing for a specific mission profile is assessed. The goal is to evaluate the energy savings and overall performance gains of optimizing the wingspan for each different mission stage by using a variable span wing, conversely to what is usually made in aircraft design, which consists of optimizing the wing for cruise conditions. There are generically, three different ways of optimizing the wing layout:

- optimizing the wingspan and wing chord for the cruise condition with possible performance limitations in all other mission stages (**fixed-wing**, **monolithic optimization**);
- globally optimizing the wingspan and wing chord so that these will be compatible in all flight stages, Table I (**fixed-wing**, **distributed optimization**);
- optimizing the wingspan for each mission stage and making sure the wing chord is the same in all flight stages, Table II (**variable-span wing**, **distributed optimization**);

Subspace optimization is also known as disciplinary optimization. This is because most of the research works on MDO have divided the problem in the classical design disciplines: aerodynamics, structures, stability, propulsion, among others, with one of the strongest motivations for multidisciplinary optimization being the aero-structural design of wings.

Unlike this classical disciplinary partitioning, the present study aiming at a comparative analysis of the aforementioned

TABLE I
FIXED WING DISTRIBUTED OPTIMIZATION PROBLEM

Stage	Input	Variables		Constraints	Objective
		Shared	Local		
(1) Take-off	-	c, b	-	Δx_{to}	E_{to}
(2) Climb	RoC		C_l	-	E_{cb}
(3) Climb	-		C_l, δ	Δt	E_{cb}
(4) Cruise	V, R		-	-	E_{cz}
(5) Cruise	V, Δt		-	-	E_{cz}
(6) Cruise	R		V	-	E_{cz}
(7) Cruise	Δt		V	-	E_{cz}
(8) Descent	-		V	R	E_{dt}

design optimization possibilities - with either fixed or variable span wing - has considered each mission stage as a different subspace.

Instead of each subspace representing a single discipline, the implemented methodology looks at each mission stage as a different subspace. There are four main mission stages: take-off, climb, cruise and descent. Each subspace will thus be associated to one of this mission stages.

Table I features a list of all possible mission stage options, each having its own set of inputs, variables, constraints and objectives for the fixed wing case, where both the wing chord (c) and wingspan (b) are shared design variables, whereas Table II does the same for the variable span wing (VSW) case, where the single shared variable is the wing chord (c).

TABLE II
VARIABLE SPAN WING DISTRIBUTED OPTIMIZATION PROBLEM

Stage	Input	Variables		Constraints	Objective
		Shared	Local		
(1) Take-off	-	c	b	Δx_{to}	E_{to}
(2) Climb	RoC		b, C_l	-	E_{cb}
(3) Climb	-		b, C_l, δ	Δt	E_{cb}
(4) Cruise	V, R		b	-	E_{cz}
(5) Cruise	V, Δt		b	-	E_{cz}
(6) Cruise	R		b, V	-	E_{cz}
(7) Cruise	Δt		b, V	-	E_{cz}
(8) Descent	-		b, V	R	E_{dt}

This multilevel optimization routine has been developed in Fortran language. The interface is made via three types of text files: inputs (where the user loads all the optimization goals and defines the mission profile), databases (with batteries/fuel, motors/engine and airfoil specifications) and outputs (including all the results and possible warnings if the inputs are not compatible with the intended mission).

V. DISCIPLINARY MODELS

First and foremost it is very important to recall that the developed methodology aims to be solving a preliminary design optimization problem. As so, the physical models described hereinafter are low fidelity ones. The idea is to rapidly have a first estimate of the relevant design variables to attain the previously defined goals.

Although XFOIL - used for the aerodynamics - cannot exactly be considered a low fidelity model in the context of low Reynolds airfoil aerodynamic evaluation, the lack of an elaborate physical model (e.g. lifting line theory, vortex lattice or 3D Panel method) means the aerodynamic, stability and overall performance assessment can be considered low fidelity models.

A. Weight

The design take-off weight (DTOW) is the sum of the aircraft structure, systems, energy and payload weights (4), where: structure refers to the structural components, like the wing, tail, fuselage and landing gear; systems refers to all devices required for flight that are not structural, such as the motor, propeller, electronic speed control (ESC), cables, servomechanisms and the receiver; energy refers to the weight of the power source used, either fuel, in the case of a combustion engine or batteries, in the electrical motor case, whereas the payload refers to all cargo and devices that might be transported by the UAV but which are not required for flight.

$$DTOW = W_{str} + W_{sys} + W_{ene} + W_{pay} \tag{4}$$

The type of propulsion, payload weight and systems weight, together with the intended mission profile are user inputs. Conversely, the structural weight will depend on the energy weight which in turn will depend on the mission profile. For a typical mission with a cruise/loiter phase the energy weight is iterated until the desired range and/or endurance are attained.

The weight formulation [1], [29] consists of an empirical approach for estimating the actual structure based on a reference structure whose main components' weights are already known.

The actual structure weight differences with respect to the reference structure makes it possible to easily infer about the structural weight impact of varying some key design variables. These include but are not limited to the airfoils' relative thickness, wing areas, aspect ratios and taper ratios as well as on the fuselage length, diameter and distance between the aerodynamic centers of the wing and the horizontal stabilizer.

Accordingly, the structural weight of the aircraft under analysis is the sum of the reference aircraft structural weight and the main structural components weight corrections (5).

$$\begin{aligned} W_{str} = & {W_{str}}^{ref} + \Delta W_w + \Delta W_{ht} + \Delta W_{vt} + \Delta W_{fus} \\ & + \Delta W_{mlg} + \Delta W_{nlg} \end{aligned} \tag{5}$$

The structural weight differences have been estimated in line with the approach followed by Gamboa et al [29], and an analogous approach was adopted for the main and nose landing gears, again based on the weight correlations of [1]. The weight variation estimates for the main structural components are shown in (6-11).

$$\Delta W_w = K_w W^{ref}\left[\left(\frac{S_w}{S_w^{ref}}\right)^{0.758}\left(\frac{\Lambda_w}{\Lambda_w^{ref}}\right)^{0.6}\left(\frac{\lambda_w}{\lambda_w^{ref}}\right)^{0.04}\left(\frac{t/c}{t/c^{ref}}\right)^{-0.3}\left(\frac{nW}{n^{ref}W^{ref}}\right)^{0.49}-1\right] \quad (6)$$

$$\Delta W_{ht} = K_{ht} W^{ref}\left[\left(\frac{S_{ht}}{S_{ht}^{ref}}\right)^{1.344}\left(\frac{\Lambda_{ht}}{\Lambda_{ht}^{ref}}\right)^{-0.448}\left(\frac{nW}{n^{ref}W^{ref}}\right)^{0.414}-1\right] \quad (7)$$

$$\Delta W_{vt} = K_{vt} W^{ref}\left[\left(\frac{S_{vt}}{S_{vt}^{ref}}\right)^{1.31}\left(\frac{\Lambda_{ht}}{\Lambda_{ht}^{ref}}\right)^{0.437}\left(\frac{nW}{n^{ref}W^{ref}}\right)^{0.376}-1\right] \quad (8)$$

$$\Delta W_{fus} = K_{fus} W^{ref}\left[\left(\frac{S_{wet}}{S_{wet}^{ref}}\right)^{1.086}\left(\frac{L}{L^{ref}}\right)^{-0.051}\left(\frac{L_{fus}/D_{fus}}{L_{fus}^{ref}D_{fus}^{ref}}\right)^{-0.072}\left(\frac{nW}{n^{ref}W^{ref}}\right)^{0.177}-1\right] \quad (9)$$

$$\Delta W_{mlg} = K_{mlg} W^{ref}\left[\left(\frac{nW}{n^{ref}W^{ref}}\right)^{0.768}\left(\frac{L_m}{L_m{}^{ref}}\right)^{0.409}-1\right] \quad (10)$$

$$\Delta W_{nlg} = K_{nlg} W^{ref}\left[\left(\frac{nW}{n^{ref}W^{ref}}\right)^{0.566}\left(\frac{L_n}{L_n{}^{ref}}\right)^{0.845}-1\right] \quad (11)$$

where (K_w), (K_{ht}), (K_{vt}), (K_{fus}), (K_{mlg}), and (K_{nlg}) are the ratios of the reference component weight to the reference vehicle's weight, for the wing, horizontal tail, vertical tail, fuselage, main landing gear and nose landing gear, respectively.

In order to guarantee the reliability of this approach, it should be assured that the actual and reference structures have similar materials, structural layout and manufacturing techniques. If that is not the case an appropriate material factor coefficient must be found to correct (6-11).

The wing weight estimates presented in (6) refer to a fixed wing. Since the aim is to be able to provide an acceptable estimate for a variable span wing as well, it is important to correct the wing structural weight estimate accordingly. Cunha [28] has developed a parametric study in ANSYS software to find a correlation for estimating the weight of a variable span wing with a given chord (c). It has been shown that the wing weight varies with the wingspan (b) and span extension factor (p), which is defined by $(p = (b_{max} - b_{min})/b_{max})$, according to (12).

$$W(p,b) = 1.4522724 + 9.666774p - 0.001604916b + 0.0003566916p^2 + 0.859356b^2 + 1.718712pb \quad (12)$$

From the fixed wing weight (W_w), it is straightforward to estimate the weight of the corresponding variable span wing (13).

$$W_w{}^{VSW} = W_w \frac{W(p,b)}{W(0,b)} \quad (13)$$

B. Propulsion

A scheme with the propulsion model for the electrical motor case is shown in Fig. 2. The thrust setting (δ) and electrical current (I) are initially guessed and thereafter iterated, while the user has to know the idle voltage $({U_{bat}}^0)$ as well as the internal resistances of the battery (R_{bat}) and the electronic speed control (ESC) device (R_{ESC}). Finally, the required power (P_{req}), is the product of the airplane drag (D) by its velocity (V) for the flight condition under study, which comes from the flight mechanics analysis and vehicle mission. Three iteration cycles have been built. One is optional and is only used if one wants to establish a maximum current and correct the thrust setting if this limit is exceeded. A second iteration cycle makes sure the electric current is corrected so that the electrical motor power (P_{mot}), equals the absorbed propeller power (P_{prop}/η_{prop}) which is a must since there is no slippage between the two. A last iteration corrects the thrust setting to ensure the available propulsive power (P_{prop}) equals the required power (P_{req}). In the diagram of Fig. 2 (η_{mot}) refers to the motor efficiency and (η_{prop}) to the propeller's efficiency.

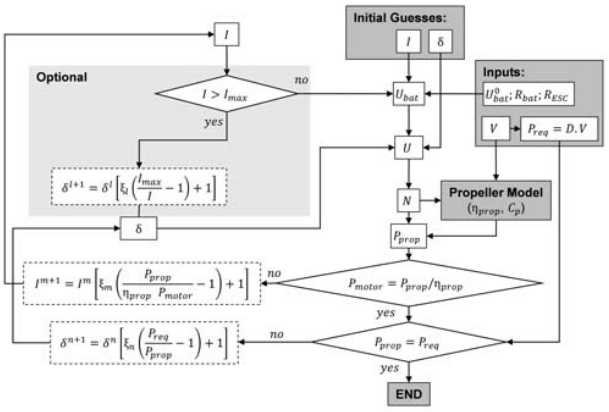

Fig. 2 Propulsion model implemented for the electrical motor case

A scheme with the propulsion model for the combustion engine case is shown in Fig. 3. The thrust setting (δ) and rotational speed (N) are initially guessed and thereafter iterated. The required power (P_{req}), is again the product of the airplane drag (D) by its velocity (V) for the flight condition under consideration. Three iteration cycles have also been built. One is optional and is only used if one wants to establish a maximum thrust setting (δ_{max}) for each mission stage. A second iteration cycle makes sure the thrust setting is such that the shaft power (P_{shaft}), equals the absorbed propeller power (P_{prop}/η_{prop}) because there is no slippage between the shaft and the propeller. A final iteration corrects the thrust setting to ensure the available propulsive power (P_{prop}) equals the required power (P_{req}). In the diagram of Fig. 3 (η_{eng}) refers to the engine efficiency and (η_{prop}) to the propeller's efficiency.

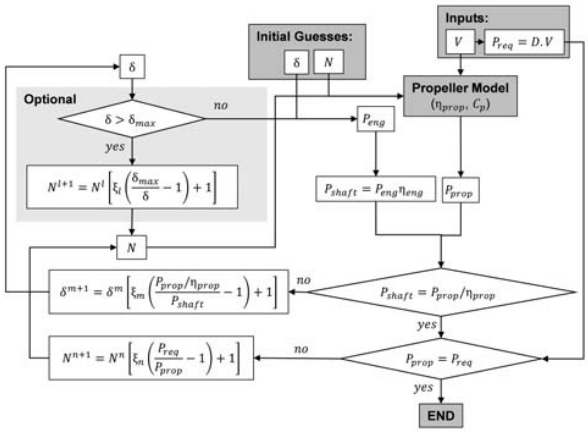

Fig. 3 Propulsion model implemented for the combustion engine case

The implemented routine needs to know how the power coefficient (C_p) and propeller efficiency (η_{prop}) vary with the propeller advance ratio (J),(14).

$$J = \frac{60V}{N.D} \tag{14}$$

Several different alternatives can be used for the propellers' performance assessment. By increasing degree of complexity, possible propeller analysis programs include: PropSelector, JavaProp and QPROP. The first is relatively straightforward to use - making use of experimental propeller data and does not need many input parameters whereas the latter has got a relatively sophisticated and accurate aerodynamic model - with an advanced Blade-Element/Vortex Method - thus requiring more input data, including detailed information regarding the propeller shape. More recently, Morgado et al [30] have implemented JBLADE which has also proven to be a reliable solution having already been bench-marked against JavaProp, QPROP and experimental data.

C. Aerodynamics

1) Lifting Surfaces: In all conventional subsonic aircraft with medium/high aspect ratio wings, the most relevant single contribution to the overall aerodynamic performance comes from the wing airfoil and therefore its careful selection is paramount. For this reason, the driving parameter of the design study is the cruise/loiter airfoil lift coefficient. This value is user defined but is bounded by the airfoils stall lift coefficient and a cruise velocity interval given by the user, according to the vehicle's operational requirements.

For the lifting surfaces' airfoils analysis, and given the low Reynolds number expected for UAV operations, the XFOIL software has been used. The user selects a number of different airfoils which are run in XFOIL for a set of Reynolds numbers, which are either interpolated or extrapolated each time an aerodynamic coefficient (either C_l, C_d or C_m) is required. In order to obtain the lifting surfaces aerodynamic coefficients (3D), the following procedure has been adopted: an iterative solution for finding both the induced angle of attack (α_i) and the 3D lift coefficient (C_L), using (15).

$$\begin{cases} \alpha_i = \frac{C_L}{\frac{\pi\Lambda}{e}} \\ C_L = C_l cos(\alpha_i) \end{cases} \tag{15}$$

The 3D drag coefficient (C_D) is the sum of the profile drag (C_d) with the lift induced drag, (16).

$$C_D = C_d + \frac{C_L^2}{\pi\Lambda e} \tag{16}$$

The Oswald span efficiency factor (e) is dependent on the wing planform geometry. Finally, and assuming a wing without twist, taper or sweep, the lifting surface pitching moment coefficient at zero lift (C_{M_0}) can be assumed equal to the airfoil pitching moment coefficient at zero lift (C_{m_0}), (17).

$$C_{M_0} \approx C_{m_0} \tag{17}$$

2) Fuselage: In order to determine the fuselage parasite drag, the equivalent skin-friction method is adopted because a well-designed aircraft in subsonic cruise will have parasite drag that is mostly skin-friction drag plus a small separation pressure drag [1]. For laminar ($Re < 1000$) and turbulent flow ($Re \geq 1000$), respectively:

$$C_f = \frac{1.328}{\sqrt{Re_x}} \tag{18}$$

$$C_f = \frac{0.455}{(\log_{10} Re_x)^{2.58}(1 + 0.144M^2)^{0.65}} \tag{19}$$

Equations (18) and (19) refer to the local friction coefficient and must be integrated along the characteristic length to obtain the total friction coefficient. Several corrections for the local Reynolds number ($Re_x = \frac{Vx}{\nu}$) may be found in Raymer [1] which account for early transition on rough surfaces. The total viscous drag can be computed from ((20)), where (q) is the dynamic pressure, (S_{wet}) the fuselage surface area (wetted area), (C_f^{total}) is the total friction coefficient, (F) is the fuselage form factor and (Q) the interference factor, which accounts for the fact that parasite drag is increased due to the mutual interference with the lifting surfaces and other components. This effect is usually negligible in the case of the fuselage ($Q = 1$) [1].

$$D_{fus} = qS_{wet}C_f^{total}FQ \tag{20}$$

The form factor (F) is a function of the fuselage characteristic dimensions [1], ((21)).

$$F = 1 + \frac{1}{\left(\frac{L_{fus}}{D_{fus}}\right)^3} + \frac{\frac{L_{fus}}{D_{fus}}}{400} \tag{21}$$

3) Miscellaneous: In what concerns to miscellaneous aerodynamic drag, it is at least worthwhile to consider the landing gear contribution for the overall drag since most unmanned aerial vehicles (UAVs) do not have retractable landing gears and they do not have streamlined shapes like the lifting surfaces or the fuselage. Its drag is best estimated by comparison to test data for a similar landing gear configurations [1]. In case that data is not available, the gear drag can be estimated as a sum of the wheels, struts and other components using typical drag coefficients for each component as featured in [1].

D. Stability

The nomenclature and signs convention used for the stability analysis is the one adopted by Etkin [31]. The tail sizing is made at each mission iteration step for the cruise velocity. In case the mission includes more than one cruise stage the cruise velocity of the first of them will be used for tail sizing purposes. The best horizontal tail arm, area and aspect ratio will depend on the cruise velocity which will vary with DTOW and will comply with the static stability requirements. The user will have to define the minimum desired static margin (K_n), ((22)), which is the distance between the CG (h) and the airplanes neutral point (h_n) all variables are non-dimensional with respect to the wing mean aerodynamic chord.

Furthermore, the CG position will be a user input, with the horizontal tail size and distance from the wing obeying the consequent neutral point position, which is fully defined as the static margin and CG positions are known.

$$K_n = h_n - h \tag{22}$$

The lateral static stability requirements must make sure that, if the sideslip (β) with respect to both the rolling and yawing movements is not null, the airplane will automatically tend to counteract such tendencies. In line with the sign and axis conventions adopted [31], it must be assured that, for the rolling maneuver - the rolling moment coefficient derivative with respect to the sideslip angle (C_{l_β}) - respects the inequality ((23)).

$$C_{l_\beta} < 0 \tag{23}$$

To make sure this requirement is met, some wing dihedral might be required. In what concerns to yawing maneuver - the yawing moment coefficient derivative with respect to the sideslip angle (C_{n_β}) - must respect the inequality ((24)).

$$C_{n_\beta} > 0 \tag{24}$$

To make sure this requirement is met, if needed the vertical stabilizer area is increased proportionally.

In what regards to the dynamic stability, no optimization procedure has been implemented. However, the longitudinal and lateral dynamic stability matrices are estimated. In order to calculate the stability derivatives that allow the computation of the matrices' eigenvalues, several theoretical and experimental correlations have been used [31]. These eigenvalues provide data on the phugoid and short-period for the longitudinal modes and rolling, spiral and dutch-roll for the lateral ones. These data enable the designer to conclude about the dynamic response of the aircraft.

VI. Case Study

To validate the implemented optimization methodology, the wing shape optimization for a specific mission is shown. The goal is to evaluate the energy savings of optimizing the wingspan for each different mission stage by using a variable span wing, conversely to what is usually made in aircraft design, which consists of optimizing the wing for cruise conditions. Fig. 4 depicts the case study mission profile. It consists of a take-off, climb, low altitude high-speed cruise, further climb to high altitude, high altitude low-speed cruise and a final descent to the take-off altitude with the goal of landing. This mission corresponds to using the mission stages (1), (2), (5), (3), (4) and (8), as defined in Table I and Table II.

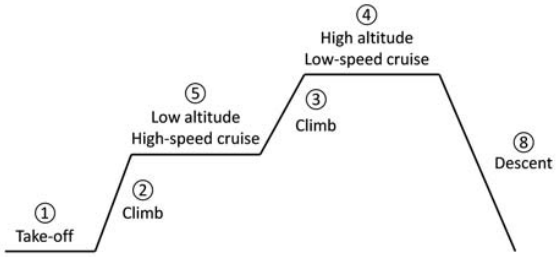

Fig. 4 Mission profile for case study

Three optimization possibilities have been considered:

- Local optimization: refers to the mathematical optimum of having the optimum wing size for each mission stage, corresponding to a physical limit and a condition which current engineering developments can not replicate;
- Global optimization (fixed wing): corresponds to a fixed-wing whose size is found by a global optimization procedure that takes into consideration all the mission stages' influence on minimizing the objective function (energy consumption);
- Global optimization (VSW): corresponds to a variable span wing global optimization procedure for finding a wing chord compatible between all mission stages, locally optimizing the wingspan for each mission stage.

The motor chosen was the Scorpion SII-4025-440KV and the propeller was the $15'' \times 8''$ as these have been considered adequate for the UAV DTOW forecast. The airfoil chosen was the SG6042. A typical specific energy value for the battery has been assumed for computing the energy weight and a safety margin of 10% has been used. The most relevant case study inputs have been summarized in Table III.

TABLE III
Input Data Parameters for the Case Study

Stage	Input Parameters
(1) Take-off	$V_{wind} = 0$, $h_{to} = 0m$
(2) Climb	$RoC = 1m/s$, $h_{min} = 0m$, $h_{max} = 250m$
(5) Cruise	$V_{min} = 35m/s$, $R = 15,000m$
(3) Climb	$\Delta t = 500s$, $h_{min} = 250m$, $h_{max} = 1,000m$
(4) Cruise	$V_{min} = 18m/s$, $\Delta t = 1,800s$
(8) Descent	$V_{min} = 20m/s$, $h_{max} = 1,000m$, $h_{min} = 0m$

Additionally, several constrains haven been added to the most relevant design variables. As for the wingspan and wing chord, the imposed limits are the ones listed in ((25)) and ((26)).

$$0.3m < c < 0.5m \tag{25}$$

$$3.0m < b < 5.0m \tag{26}$$

The initial guesses - the starting point for iterating - were ($c = 0.4m$) and ($b = 4.0m$). Moreover the payload and systems weight have been established as ($W_{pay} = 15N$) and ($W_{sys} = 15N$), respectively, although the systems weight will have a penalty in the VSW case (to account with the servomechanism). Conversely, the structural (W_{str}) and energy weight (W_{ene}) will be estimated and updated throughout the optimization process.

VII. Results

The optimum wing shape (wing chord, wingspan) combination for each optimization conditions are summarized in Table IV.

TABLE IV
Optimum Wing Shape for Each Mission Stage According to the Optimization Method [m]

Stage	Local Optimum		Global Optimum (fixed wing)		Global (VSW)	
	c	b	c	b	c	b
①	0.50	5.00	0.38	3.92	0.39	5.00
②	0.39	4.23				5.00
⑤	0.30	3.00				3.00
③	0.44	4.70				4.96
④	0.33	3.00				3.62
⑧	0.40	4.00				4.00

The graphical representations of Figs. 5 and 6 provide an easy way of comparing the optimum wing shapes for each mission stage in the VSW case and the global fixed wing optimum shape. It is interesting to note that although the optimum wing chords are similar in the two cases ($c_{fixed} = 0.38m$) and ($c_{vsw} = 0.39m$), the optimum wingspan for each mission stage featured in Fig. 6 are significantly different. As expected, the lowest VSW wingspan correspond to the first cruise condition, the one with the highest operational velocity.

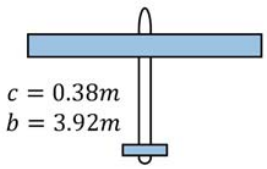

Fig. 5 Optimized fixed wing shape for the defined mission profile

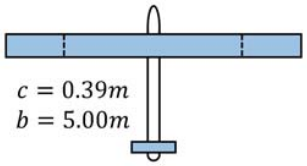

(a) Take-off configuration

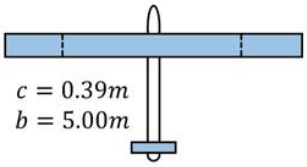

(b) First climb configuration

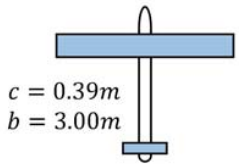

(c) First cruise configuration

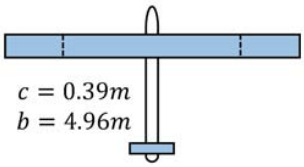

(d) Second climb configuration

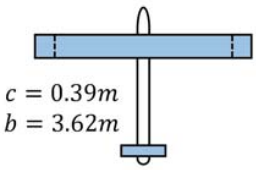

(e) Second cruise configuration

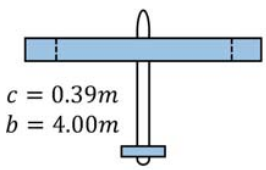

(f) Descent configuration

Fig. 6 Optimized VSW shape for each mission stage

The energy consumption at each mission stage, depending on the optimization approach, are presented in Table V. The

first column is just shown for benchmarking purposes as it refers to the mathematical optimum - it is not possible to have a different wingspan, wing chord combination at each mission stage. Conversely, the other two columns deserve more attention as they are the actual energy consumptions for the multidisciplinary and multilevel distributed (or global) design optimization architectures. The second column refers to the fixed wing and the third to the VSW.

TABLE V
ENERGY CONSUMPTION IN EACH MISSION STAGE DEPENDING ON THE OPTIMIZATION METHOD EMPLOYED [J]

Stage	Local Optimum	Global Optimum (fixed wing)	Global Optimum (VSW)
①	1,766	2,268	2,569
②	62,175	63,099	72,806
⑤	228,801	308,063	266,886
③	159,695	161,342	191,067
④	169,248	264,681	199,312
⑧	0	0	0
Total	621,685	799,453	729,640

For this case study's mission profile, the overall energy savings of using a VSW were found to be over 8.7%. This is a remarkable difference, particularly if it is taken into account that the aircraft DTOW for the fixed wing UAV is estimated at $(87N)$, whereas in the VSW case it is almost $(110N)$. This weight differences account for energy, systems and structural weight, since the payload is the same in both cases and equal to $(15N)$. While the fixed-wing case energy weight is estimated in about $(17.1N)$, the VSW is only $(15.6N)$. Conversely, the structural weight will be significantly higher on the VSW $(61N)$, being only $(40N)$ for the fixed wing case. Finally, for the systems weight, there is a penalty of about $(3N)$ for the VSW to account for the VSW servomechanisms.

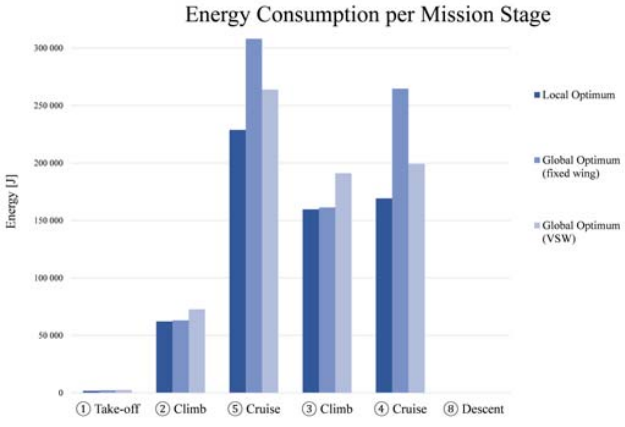

Fig. 7 Energy consumption [J] per mission stage for the three optimization conditions considered

It is interesting to note in Fig. 7 how the VSW has a negative impact on the mission stages with the lowest overall energy consumption. This happens because of the already discussed DTOW increase for the VSW. However it is important to mention that the overall energy consumption on the VSW is lower as its improved performance on the cruise mission stages outweighs the discussed negative impact of the increased DTOW. As for the descent mission stage, the airfoil lift coefficient will be corrected to make sure the energy consumption is null in all the cases considered.

Finally, it is worthwhile to note that had the weighting coefficient (λ_w^i) concept not been introduced, both optimizations would generate worse results. The weighting of the subspaces is paramount for an enhanced optimization. If a similar weighting would be assigned to mission stages with significantly different energetic impact on the overall energy consumption the multilevel optimization methodology would be skewed.

VIII. CONCLUSIONS

A comprehensive multidisciplinary and multilevel morphing wing aircraft design methodology using the Enhanced Collaborative Optimization architecture has been implemented and the results of a case study have been shown and discussed. The modularity of the routine developed allows it to be easily modified to either choose a different mission pattern each time it is run, improve the fidelity of its physical models and/or widen the morphing technologies considered, unfolding novel approaches in the context of preliminary design optimization.

In spite of using the original ECO formulation [15], two slight modifications were made: the use of a weighting coefficient (λ_w^i) for the system level optimization and a dynamic compatibility parameter (λ_c^*) for the subspace level optimization.

The weighting coefficient (λ_w^i) will multiply the squared difference between the subspaces best attempt to match the system level targets (x^*) and the system level targets (z) themselves which enables the user to assign a different relative weight to each subspace solution within the overall optimization. As the main goal of the case study presented is to minimize the overall energy spent, it results obvious that a more optimized result can be reached if more relevance is given to the mission stages (subspaces) with the highest energy consumptions.

It has also been found that the use of a dynamic compatibility parameter (λ_c^*) instead of a constant one can actively contribute to avoid early constraints to the subspaces optimizations that can jeopardize the quest for minimization. Indeed, a constant compatibility parameter in the first system level iterations can have a negative impact on the local optimization functions by forcing a premature compatibility between subspaces that may put the optimization process at risk. It has been witnessed that the best results were achieved when the compatibility parameter was zero on the first system level iterations, only assuming a positive definite value after a threshold number of iterations - this threshold being problem dependent.

The case study presented clearly shows that albeit the overall structural and systems weight increase due to the use of a variable wing span mechanism, it is advantageous to use

it for improving the overall aircraft performance so long as the appropriate wingspan is in use in each different mission stage. It is interesting to note that this energy savings in a preliminary design context can outweigh the ones obtained by an enhanced detailed design of the motors/engines or airfoils, meaning that multilevel and multidisciplinary design optimization can be as important as - if not more in some cases - than advanced disciplinary optimizations.

Nevertheless, it is worthwhile to mention that the general quantitative gain of using a VSW optimized with a multilevel distributed architecture is impossible to forecast as it is highly dependent on the intended mission profile. In same cases, the use of a VSW might proof of little relevance or even have a negative performance impact whereas in other cases, namely the ones with at least two different mission stages with a significant energy consumption, the impact shall be highly positive.

IX. Future Work

The forthcoming steps include the application of this methodology using a different multilevel optimization architecture than the ECO for benchmarking purposes and using a sampling and/or heuristics optimization algorithm or a mixed heuristic-genetic algorithm instead of a gradient-based one. Additional enhancements may include addressing the fidelity of the physical models as well as the development of a graphical user interface.

Acknowledgment

The work presented herein has been partially funded by the European Communitys Seventh Framework Programme (FP7) under the Grant Agreement 314139. The CHANGE project (Combined morphing assessment software using flight envelope data and mission based morphing prototype wing development) is a Level 1 project funded under the topic AAT.2012.1.1-2. involving 9 partners. The project started on August, 2012.

References

[1] D. P. Raymer, *Aircraft Design: A Conceptual Approach*. AIAA, 1989.

[2] R. T. Haftka, J. Sobieszczanski-Sobieski, and S. L. Padula, "On Options for Interdisciplinary Analysis and Design Optimization," *Structural Optimization*, vol. 4, p. 6574, 1992.

[3] E. J. Cramer, J. E. Dennis Jr., P. D. Frank, and a. S. G. R. Lewis, R. M., "Problem Formulation for Multidisciplinary Optimization," *SIAM Journal on Optimization*, vol. 4, no. 4, p. 754776, 1994.

[4] R. J. Balling and J. Sobieszczanski-Sobieski, "Optimization of Coupled Systems: A Critical Overview of Approaches," *AIAA Journal*, vol. 34, no. 1, p. pp. 617, 1996.

[5] N. Alexandrov and M. Y. Hussaini, "Multidisciplinary Design Optimization: State-of-the-Art," *SIAM*, 1997.

[6] I. M. Kroo, ""MDO for Large-Scale Design Multidisciplinary Design Optimization: State-of-the-Art," *edited by N. Alexandrov and M. Y. Hussaini SIAM*, p. pp. 2244, 1997.

[7] N. M. Alexandrov, "Multilevel Methods for MDO," *Multidisciplinary Design Optimization: State-of-the-Art, edited by N. M. Alexandrov and M. Y. Hussaini SIAM*, 1997.

[8] R. J. Balling *Multidisciplinary Design Optimization: State-of-the-Art, edited by N. M. Alexandrov and M. Y. Hussaini, SIAM*, no. 1.

[9] S. J. Sobieszczanski and R. T. Haftka, "Multidisciplinary Aerospace Design Optimization: Survey of Recent Developments," *Structural Optimization*, vol. 14, no. 1, p. pp. 123, 1997.

[10] J. R. R. A. Martins and A. B. Lambe, "Multidisciplinary Design Optimization: A Survey of Architectures," *AIAA Journal*, vol. 51, pp. 2049–2075, 2013.

[11] Weisshaar, Terrence A., "Morphing Aircraft Technology New Shapes for Aircraft Design," 2006.

[12] S. Barbarino, O. Bilgen, R. Ajaj, M. Friswell, and D. Inman, "A Review of Morphing Aircraft," *Journal of Intelligent Material Systems and Structures*, vol. 22, pp. pp. 823–877, 2011.

[13] S. Joshi, Z. Tidwell, W. Crossley, and S. Ramakrishnan, "Comparison of Morphing Wing Strategies Based Upon Aircraft Performance Impacts," *45th AIAA/ASME/ASCE/AHS/ASC Structures, Structural Dynamics and Materials Conference*, 2004.

[14] P. F. Albuquerque, P. V. Gamboa, and M. A. Silvestre, "Parametric Aircraft Design Optimisation Study Using Span and Mean Chord as Main Design Drivers," *Advanced Materials Research*, vol. 1016, pp. 365–369, 2014.

[15] B. Roth and I. Kroo, "Enhanced Collaborative Optimization: Application to an Analytic Test Problem and Aircraft Design," *12th AIAA/ISSMO Multidisciplinary Analysis and Optimization Conference, Victoria, BC, Canada*, 2008.

[16] B. Roth and I. Kroo, "Enhanced Collaborative Optimization: A Decomposition-Based Method for Multidisciplinary Design," *ASME 2008 International Design Engineering Technical Conferences Computers and Information in Engineering Conference, IDETC/CIE 2008*, 2008.

[17] B. D. Roth, "Aircraft Family Design Using Enhanced Collaborative Optimization," Master's thesis, Stanford University, 2008.

[18] I. M. Kroo, S. Altus, R. Braun, P. Gage, and I. Sobieski, "Multidisciplinary Optimization Methods for Aircraft Preliminary Design," *5th AIAA/USAF/NASA/ISSMO Symposium on Multidisciplinary Analysis and Optimization*, 1994.

[19] S. Kodiyalam, "Evaluation of Methods for Multidisciplinary Design Optimization (MDO), Phase I," *Tech. Rep. CR-1998-208716, NASA*, 1998.

[20] S. Kodiyalam and C. Yuan, "Evaluation of Methods for Multidisciplinary Design Optimization (MDO), Part 2," *Tech. Rep. CR-2000-210313, NASA*, 2000.

[21] A. J. de Wit and F. van Keulen, "Numerical Comparison of Multi-level Optimization Techniques," *AIAA/ASME/ASCE/AHS/ASC Structures, Structural Dynamics, and Materials Conference, Honolulu, HI*, 2007.

[22] S. I. Yi, J. K. Shin, and G. J. Park, "Comparison of MDO Methods with Mathematical Examples," *Structural and Multidisciplinary Optimization*, vol. 39, p. 391402, 2008.

[23] X. Mi, Q. Haobo, G. Liang, S. Xinyu, and C. Xuezheng, "An Enhanced Collaborative Optimization Methodology for Multidisciplinary Design Optimization," *The State Key Laboratory of Digital Manufacturing Equipment and Technology, Huazhong University of Science and Technology, P.R.China*, 2010.

[24] P. Spellucci, "A SQP method for general nonlinear programs using only equality constrained subproblems," *Math. Prog.*, vol. 82, pp. 413–448, 1998.

[25] P. Spellucci, "A new technique for inconsistent problems in the SQP method. Math. Meth. of Oper. Res," *Math. Meth. of Oper. Res.*, vol. 47, pp. 355–400, 1998.

[26] J. R. C. Mestrinho, P. V. Gamboa, and P. D. Santos, "Design Optimization of a Variable-Span Morphing Wing for a Small UAV," *52nd AIAA/ASME/ASCE/AHS/ASC Structures, Structural Dynamics, and Materials (and co-located) Conferences, Denver, Colorado, USA*, 2011.

[27] J. Felício, P. D. Santos, P. V. Gamboa, and M. A. R. Silvestre, "Evaluation of a Variable-Span Morphing Wing for a Small UAV," *52nd AIAA/ASME/ASCE/AHS/ASC Structures, Structural Dynamics, and Materials (and co-located) Conferences, Denver, Colorado, USA*, 2011.

[28] R. Cunha, "Structural Analysis of a Variable-span Wing-box," Master's thesis, University of Beira Interior, 2014.

[29] P. V. Gamboa, M. A. Silvestre, and P. F. Albuquerque, "Aircraft Design Methodology Using Span and Mean Wing Chord as Main Design Parameters," *International Conference in Engineering of University of Beira Interior, Covilhã, Portugal*, 2013.

[30] J. Morgado, M. A. Silvestre, and J. C. Páscoa, "Validation of New Formulations for Propeller Analysis," *Journal of Propulsion and Power*, 2014.

[31] B. Etkin, *Dynamics of Flight - Stability and Control*. John Wukey Cons, Inc, 1996.